COMPUTATIONAL FLUID DYNAMICS ANALYSIS OF THE OSCILLATORY FLOW IN A JET PUMP: THE INFLUENCE OF TAPER ANGLE

OOSTERHUIS*,[1] Joris P., BÜHLER[1] Simon, WILCOX[2] Douglas and VAN DER MEER[1] Theo H.

[1]Department of Thermal Engineering, University of Twente, The Netherlands
[2]Chart Inc., Troy, NY, United States
*j.p.oosterhuis@utwente.nl

Abstract: *A two-dimensional CFD model for predicting the oscillating flow through a jet pump is developed. Various taper angles are investigated and total minor loss coefficients are derived. A good correspondence is achieved with experimental results from the literature. However, at higher taper angles a dramatic decay in the jet pump pressure drop is observed, which serves as a starting point for the improvement of jet pump design criteria for compact thermoacoustic applications.*

1. Introduction

A jet pump is a crucial part of most closed-loop thermoacoustic devices. In such devices, a time-averaged mass flux known as Gedeon streaming can exist [1]. This time-averaged mass flux results in convective heat transport that can degrade the efficiency of thermoacoustic devices. To suppress Gedeon streaming, a jet pump can be used. Backhaus and Swift have shown that by correctly shaping a jet pump it is possible to take advantage of asymmetry in hydrodynamic end effects to impose a pressure drop across the jet pump [2]. A typical jet pump consists of a narrowed, tapered tube section as shown schematically in Figure 1. By balancing the pressure drop across the jet pump with that which exists across the regenerator in a thermoacoustic device, it is possible to suppress Gedeon streaming.

Despite the proven effectiveness of jet pumps, there is a lack of understanding about the exact fluid dynamics that lead to the observed pressure drop. Current criteria for the design of a jet pump assume that the flow at any point in time has little "memory" of its past history – which is often referred to as the "Iguchi-hypothesis" – allowing the acoustic behavior to be based on a quasi-steady approximation and the use of minor loss coefficients reported for steady flow conditions [2, 3, 4, 5]. Qualitative evidence exists which supports the current analysis theory, but quantitative agreement between the theory and experiments remains poor.

Previous studies include mainly experimental work and only a few computational studies have been published. Petculescu and Wilen measured the pressure drop for a series of jet pump geometries and derived minor loss coefficients [6]. They reported a difference between the measured and theoretical minor loss coefficients. Nevertheless, for the investigated geometries – up to a taper angle of 10° – good agreement between steady flow and oscillating experiments was obtained. Computational studies related to jet pumps mainly include the work of Boluriaan and Morris [7, 8]. Although the flow field was calculated for a fixed geometry and wave amplitude, the relation between wave amplitude and pressure drop was not published.

In this paper, the oscillating flow in the vicinity of a jet pump is investigated using a computational fluid dynamics (CFD) model. Validation is provided with the experimental results of Petculescu and Wilen [6]. Furthermore, the influence of the jet pump taper angle is analyzed by changing the jet pump length. This study shows the effect on the achieved pressure drop when making a jet pump more compact.

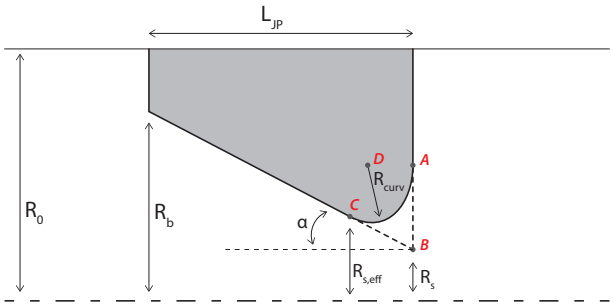

Figure 1: Jet pump with parameters that define the geometry (not to scale). Dashed line indicates centerline.

2. Modeling

A two-dimensional axisymmetric model of a jet pump is developed using the commercial CFD package COMSOL Multiphysics v4.4 [9]. To allow for the validation of the computational model, the jet pump dimensions and boundary conditions are based on data from the literature [6]. In all cases, air at a mean temperature of $T_0 = 20\,°\text{C}$ and a mean pressure of $p_0 = 1\,\text{atm}$ is used as the working fluid. The driving frequency of the system is $f = 100\,\text{Hz}$. Under these conditions, the viscous penetration depth is: $\delta_\nu = \sqrt{2\mu/\omega\rho} = 0.22\,\text{mm}$.

Geometry The jet pump geometry is defined using a number of parameters: the big radius R_b, the effective small radius $R_{s,eff}$, the taper half-angle α and the radius of curvature at the small exit of the jet pump R_{curv}. All these parameters are shown in Figure 1, with R_s being the small radius of the jet pump without curvature ($R_{curv} = 0$), as defined in Equation 1:

$$R_s = R_{s,eff} - R_{curv}\left(\frac{\sin\alpha + 1}{\cos\alpha} - \cos\alpha\right) \tag{1}$$

The total length of the jet pump is calculated using Equation 2:

$$L_{JP} = \frac{R_b - R_s}{\tan\alpha} \tag{2}$$

Besides jet pump region, the computational domain comprises a region on both sides of the jet pump with length $L_{in} = 650\,\text{mm}$ and radius R_0. The geometrical parameter values used for the validation case are listed in Table 1a.

For the simulations with variable taper angle, the exit radii R_b and $R_{s,eff}$ are kept constant and are identical to those in the validation case. By changing the jet pump length L_{JP}, the taper angle α will change and the effect of a more compact jet pump can be studied. The taper angles that are considered and resulting jet pump lengths are summarized in Table 1b.

Numerical model Within the described computational domain, the unsteady, incompressible Navier-Stokes equations are solved [9]. To solve these equations, the fully coupled direct MUMPS solver is used with a maximum time-step of $\Delta t = 1 \cdot 10^{-5}$ s. This yields $N_t = 1000$ time-steps per wave period. Additional isotropic diffusion of $\delta_{id} = 0.1$ is used to damp out initial transients and to obtain a stable solution. The assumption of incompressibility is justified by the ratio of the jet pump dimension to the acoustic wavelength: the jet pump length is much smaller than the acoustic wavelength ($L_{JP}/\lambda \ll 1$). Hence, the flow can be considered locally incompressible [10].

Parameter	Value
R_0	7.9 mm
R_b	4.04 mm
$R_{s,eff}$	0.93 mm
R_{curv}	1.85 mm
L_{JP}	27.5 mm

(a) Jet pump dimensions for validation case, based on [6].

α [°]	L_{JP} [mm]	α [°]	L_{JP} [mm]
3	64.3	15	12.6
5	38.5	20	9.3
7	27.5	30	5.8
10	19.1	45	3.4

(b) Resulting jet pump length L_{JP} for applied taper angles α.

Table 1: Dimensions of simulated jet pump geometries.

To simulate an acoustic wave inside the computational domain, an oscillating velocity boundary condition is used on the left side of the domain with $u(t) = u_1 \cdot \sin(2\pi f t)$. On the right side of the domain, a pressure boundary condition is used with a constant relative pressure of $p = 0\,\text{Pa}$ to simulate an open end. No-slip wall boundary conditions are applied to both the tube wall and the jet pump wall. On the x-axis, an axisymmetric boundary condition is imposed.

Computational mesh The domain is discretized using a computational mesh consisting of 54,000 quadrilateral elements. An unstructured mesh is used near the jet pump, combined with a structured mesh in the far field. The elements are stretched in the direction of wave propagation, corresponding to the expected gradients [11]. Moreover, a mesh refinement is applied near all no-slip wall boundaries such that a total of $N_{bl} = 10$ elements exist within a distance of a viscous penetration depth δ_ν from the wall. A further refinement to $N_{bl} = 20$ elements showed a deviation in the mean pressure drop of less than $0.2\,\%$, which provides evidence for the mesh independence of the results.

Minor loss calculation Backhaus and Swift were the first to derive an equation for the mean pressure drop across a jet pump based on steady-flow minor loss coefficients [2]. The minor losses in steady flow can be calculated using: $\Delta p_{ml} = K \frac{1}{2} \rho u^2$, with K the minor loss coefficient dependent on the geometry and, in this case, $u(t) = u_1 \sin \omega t$ a pure sinusoidal flow velocity. By time-integration, a relation for the mean pressure drop across the jet pump can be derived:

$$\Delta p_{2,JP} = \frac{1}{8} \rho_0 |u_1|^2_{JP} \left[(K_{exp,s} - K_{con,s}) + \left(\frac{A_s}{A_b} \right)^2 (K_{con,b} - K_{exp,b}) \right] \tag{3}$$

where K_{con} and K_{exp} are the minor loss coefficients for the contraction and expansion phase, respectively, and $|u_1|_{JP}$ is the maximum velocity amplitude at the small exit of the jet pump. In the current paper, the mean pressure drop as a function of $|u_1|_{JP}$ is studied. Hence, it is possible to derive a "total" minor loss coefficient, incorporating the expansion and contraction effects at both exits:

$$K_{tot} = \frac{8 \Delta p_{2,JP}}{|u_1|^2_{JP} \rho_0} \tag{4}$$

The total minor loss coefficient will be derived from the simulation results based on Equation 4. The use of more advanced models that correct for the non-harmonic velocity inside the jet pump is beyond the scope of this brief paper.

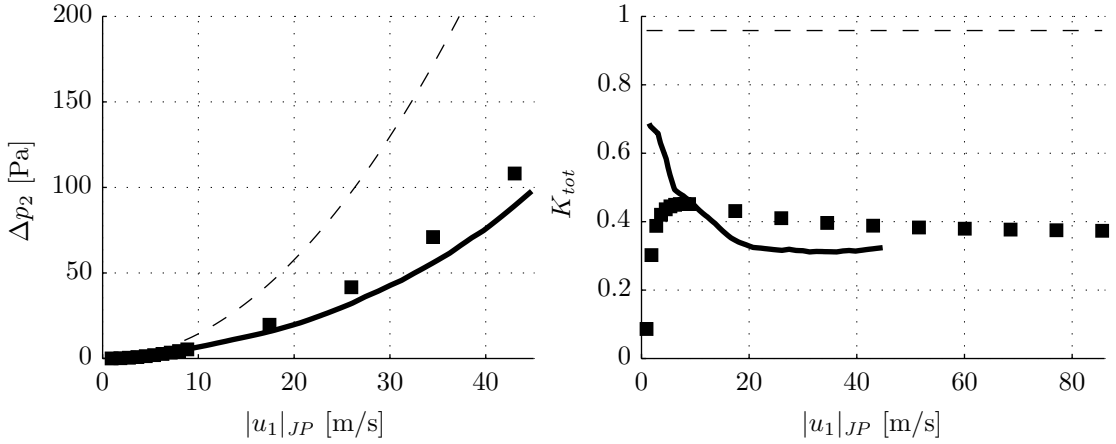

(a) Mean pressure drop Δp_2.

(b) Total minor loss coefficient K_{tot}.

Figure 2: Results of validation case, taper angle $\alpha = 7°$. Solid lines indicate results derived from [6], black squares (■) indicate simulation results and dashed lines are predictions using Eq. 3.

3. Results

The CFD model is validated by performing a range of simulations applying the reference geometry (see Table 1a). The velocity amplitude at the left boundary condition is varied from $|u_1| = 0.01$ m/s to 1.0 m/s. The resulting mean pressure drop is shown in Figure 2a. In Figure 2b, the behavior of K_{tot} as a function of the velocity amplitude is shown for both the reference data and the simulation results. It is clear that the regime where $\Delta p_2 \propto |u_1|^2_{JP}$ is only present at higher wave amplitudes, which is in accordance with earlier work [6]. A least-square fit based on Eq. 4 yields $K_{tot} = 0.32$ for the reference data and $K_{tot} = 0.38$ for the simulation results, while the theoretical total minor loss coefficient, calculated using Eq. 3, is $K_{tot} = 0.96$.

Influence of taper angle Starting from the previously used geometry, a set of simulations is carried out in which the jet pump taper angle – and consequently the jet pump length – is varied (see Table 1b). A fixed velocity amplitude of $|u_1| = 0.2$ m/s is used. A clear effect of the taper angle on the total minor loss coefficient K_{tot} is observed as shown in Figure 3: an increased taper angle leads to a decreased minor loss coefficient and thus to a decreased jet pump performance. Note that K_{tot} from simulation results is now based on a fixed velocity amplitude. These results are similar to those reported in the literature for the range of $\alpha = 3°$ to $10°$, but show a dramatic decay in K_{tot} for higher taper angles: from $\alpha = 20°$ on, no positive mean pressure drop was measured at all. This behavior is confirmed by studying the vorticity field: while for low taper angles the vortices propagate purely rightwards, at higher taper angles the vortex shedding becomes symmetric and vortices propagate in both directions. A detailed study of the vortex shedding and flow separation will be reported in a future publication.

4. Conclusion

A CFD model for the oscillating flow through a jet pump is developed and compared with earlier work. Total minor loss coefficients have been calculated, and in comparison to the theoretical values there is good agreement between simulation results and reference data. The effect of the taper angle has been studied, and for small taper angles the simulation results are equivalent to those reported in the literature. Moreover, for higher taper angles a dramatic decay in K_{tot} is

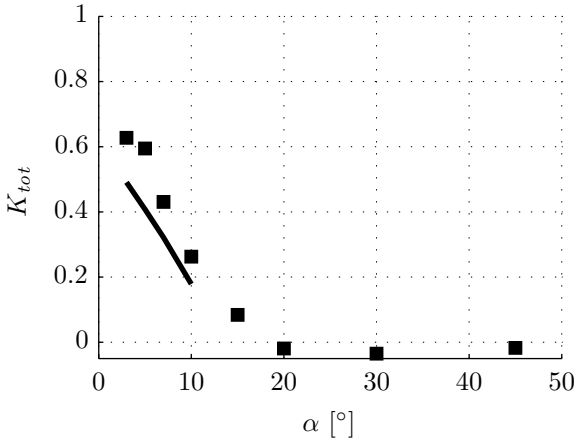

Figure 3: Effect of taper angle α on total minor loss coefficient K_{tot} for $|u_1|_{JP} = 0.2$ m/s. Solid line indicates results derived from [6], black squares (■) indicate simulation results.

observed which had not previously been reported. This certainly puts a price on the achievable pressure drop for compact jet pump designs.

The presented CFD model serves as a starting point for the numerical calculation of minor loss coefficients and a further validation of the used numerical methods will be carried out. Future research will focus both on a detailed explanation of the observed flow phenomena and on improved jet pump design criteria for compact thermoacoustic applications.

References

[1] Gedeon, D.: DC gas flows in Stirling and pulse-tube cryocoolers. *Cryocoolers* 9, 385–392 (1997)

[2] Backhaus, S. and Swift, G.: A thermoacoustic-Stirling heat engine: detailed study. *The Journal of the Acoustical Society of America* 107, 3148–3166 (2000)

[3] Iguchi, M., Ohmi, M., and Meagawa, K.: Analysis of free oscillating flow in a U-shaped tube. *Bulletin of the JSME* 25, 1398–1405 (1982)

[4] Swift, G., Gardner, D., and Backhaus, S.: Acoustic recovery of lost power in pulse tube refrigerators. *Journal of the Acoustical Society of America* 105, 711–724 (1999)

[5] Thurston, G.: Nonlinear acoustic properties of orifices of varied shapes and edge conditions. *The Journal of the Acoustical Society of America* 992, 2–5 (1958)

[6] Petculescu, A. and Wilen, L. A.: Oscillatory flow in jet pumps: Nonlinear effects and minor losses. *The Journal of the Acoustical Society of America* 113, 1282–1292 (2003)

[7] Boluriaan, S. and Morris, P. J.: Suppression of traveling wave streaming using a jet pump. In *41st AIAA Aerospace Sciences Meeting & Exhibit*. American Institute of Aeronautics and Astronautics, Reno, NY (2003)

[8] Morris, P., Boluriaan, S., and Shieh, C.: Numerical simulation of minor losses due to a sudden contraction and expansion in high amplitude acoustic resonators. *Acta Acustica united with Acustica* 90, 393–409 (2004)

[9] COMSOL: *COMSOL Multiphysics Reference Guide*. COMSOL (2012)

[10] Nakiboğlu, G.: *Aeroacoustics of corrugated pipes*. Phd thesis, Eindhoven University of Technology (2012)

[11] Bühler, S., Wilcox, D., Oosterhuis, J. P., and van der Meer, T. H.: Calculation of thermoacoustic functions with computational fluid dynamics. *Proceedings of Meetings on Acoustics* 19, (2013)